forests

MDPI

Article

Multiple-Temporal Scale Variations in Nighttime Sap Flow Response to Environmental Factors in *Ficus concinna* over a Subtropical Megacity, Southern China

Muhammad Hayat [1], Chunhua Yan [1], Jiao Xiang [1], Bowen Xiong [1], Longjun Qin [1], Alamgir Khan [2], Bei Wang [1], Mohsin Khan [3], Zhendong Zou [1] and Guoyu Qiu [1,*]

[1] School of Environment and Energy, Peking University Shenzhen Graduate School, Shenzhen 518055, China; muhammadhayat66@gmail.com (M.H.); yanch@pku.edu.cn (C.Y.); fpxj@163.com (J.X.); 18292877339@163.com (B.X.); qinlongjun@pku.edu.cn (L.Q.); wang-bei@pku.edu.cn (B.W.); zouzd@pku.edu.cn (Z.Z.)
[2] Department of Forestry, Shaheed Benazir Bhutto University, Sheringal Dir Upper 25000, KPK, Pakistan; alamgir.forester@gmail.com
[3] School of Environment, Tsinghua University, Beijing 100084, China; mohsinqau22@gmail.com
* Correspondence: qiugy@pkusz.edu.cn

Abstract: With ongoing climate change and rapid urbanization, the influence of extreme weather conditions on long-term nocturnal sap flow (Q_n) dynamics in subtropical urban tree species is poorly understood despite the importance of Q_n for the water budgets and development plantation. We continuously measured nighttime sap flow in *Ficus concinna* over multiple years (2014–2020) in a subtropical megacity, Shenzhen, to explore the environmental controls on Q_n and dynamics in plant water consumption at different timescales. Nocturnally, Q_n was shown to be positively driven by the air temperature (T_a), vapor pressure deficit (VPD), and canopy conductance (expressed as a ratio of transpiration to VPD), yet negatively regulated by relative humidity (RH). Seasonally, variations in Q_n were determined by VPD in fast growth, T_a, T/VPD, and meteoric water input to soils in middle growth, and RH in the terminal growth stages of the trees. Annual mean Q_n varied from 2.87 to 6.30 kg d^{-1} with an interannual mean of 4.39 $\pm$ 1.43 kg d^{-1} ($\pm$ standard deviation). Interannually, the key regulatory parameters of Q_n were found to be T_a, T/VPD, and precipitation (P)-induced-soil moisture content (SMC), which individually explained 69, 63, 83, and 76% of the variation, respectively. The proportion of the nocturnal to the total 24-h sap flow (i.e., $Q_n/Q_{24\text{-}h} \times 100$) ranged from 0.18 to 17.39%, with an interannual mean of 8.87%. It is suggested that high temperatures could increase transpirational demand and, hence, water losses during the night. Our findings can potentially assist in sustainable water management in subtropical areas and urban planning under increasing urban heat islands expected with future climate change.

Keywords: climate change; *Ficus concinna*; high temperature; multiple timescales; nocturnal sap flow; regulatory parameters

check for updates

Citation: Hayat, M.; Yan, C.; Xiang, J.; Xiong, B.; Qin, L.; Khan, A.; Wang, B.; Khan, M.; Zou, Z.; Qiu, G. Multiple-Temporal Scale Variations in Nighttime Sap Flow Response to Environmental Factors in *Ficus concinna* over a Subtropical Megacity, Southern China. *Forests* **2022**, *13*, 1059. https://doi.org/10.3390/f13071059

Academic Editor: Alessio Giovannelli

Received: 21 May 2022
Accepted: 2 July 2022
Published: 5 July 2022

Publisher's Note: MDPI stays neutral with regard to jurisdictional claims in published maps and institutional affiliations.

Copyright: © 2022 by the authors. Licensee MDPI, Basel, Switzerland. This article is an open access article distributed under the terms and conditions of the Creative Commons Attribution (CC BY) license (https://creativecommons.org/licenses/by/4.0/).

1. Introduction

Global warming and rapid urbanization are expected to intensify urban heat islands (UHIs) and frequent extreme weather conditions, e.g., heavy precipitations, droughts, and heatwaves [1]. During the 21st century, the first decade was observed as the warmest, and the forecasted increase in the global average surface air temperature is expected to be varied between 2 and 4 °C by 2040 [2,3], which may further increase the temperature in urban areas. The larger increases are observed in nighttime rather than daytime temperatures, especially in the tropics [4]. This warming asymmetry mainly happens by changing the levels of cloud cover. Increased cloud cover cools the surface during the day and retains the warmth at night, leading to a more significant increase in the nighttime temperature.

Consequently, the higher nighttime temperature increases the nighttime vapor pressure deficit (VPD) and decreases the relative humidity (RH), leading to an elevated atmospheric demand for water [5]. These temperature differences may certainly affect the movement of water fluxes over plants and lead to higher nighttime transpiration (T) rates [6,7]. In addition, the nocturnal water use may have, in turn, modified the daily balance of water consumption by local vegetation [8]. Nighttime sap flow (Q_n) has an effect not only on the local to regional water balances but also on the vegetation response to nutrient and water shortage (e.g., resilience and resistance) with ongoing climate change [9]. Furthermore, Q_n provides benefits for plants such as the prevention of surplus leaf turgor at night [10], acceleration of nutrient acquisition [11], transport of O_2 to xylem parenchyma [12], enhanced CO_2 assimilation and advanced stomatal opening in the early morning [13]. In these circumstances, nighttime plant water-consumption dynamics and patterns recently have become a focus of attention for the sustainable management of ecologically important plants in urban areas.

In the past, it was generally presumed that low nighttime stomatal conductance, low VPD, and the absence of sunlight caused no transpiration or was very small at night [14,15]. Nowadays, there is growing proof that stomata remain partially open at night, reinforcing a non-trivial level of Q_n in various plant species and ecosystems [5,10,16,17]. Previous studies documented that nighttime water loss and high stomatal aperture have been globally predicted to increase nighttime transpiration and exacerbate soil water deficits [18,19]. Furthermore, the documented contributions of Q_n to total daily ($Q_{24\text{-}h}$) water consumption of vegetation is highly variable with species and biomes [9,20]. For instance, over a wide range of habitats, the contribution ratio (i.e., $Q_n/Q_{24\text{-}h} \times 100\%$) is varied between 1% and 28% [6]; however, values up to 30–60% with an average of 12% have also been observed [18,21]. A higher ratio of Q_n was observed in species that were less disposed to soil and atmospheric water scarcity or for wet areas (i.e., rainforests) [22]. Likewise, the Q_n rate in trees significantly increases instantly after rainfall following low water conditions, further affecting the water balances [4]. However, there is limited research on Q_n, despite the importance of estimating the water balances and vegetation's functioning in an urban thermal environment.

Regarding large heterogeneous environmental conditions in the subtropical urban areas, the on-site hydrometeorological regulating parameters of Q_n can be varied markedly within a very short interval, which might affect the nighttime water usage of plants differently across temporal scales [23,24]. Generally, air temperature (T_a), VPD, wind speed (W_s), precipitation (P), soil moisture content (SMC), and canopy conductance (as indicated by T/VPD) are the most important parameters influencing plant water fluxes and growth [25–29]. It has been documented that Q_n is positively correlated to T_a and VPD at short timescales, e.g., nocturnally [30,31], and with SMC at longer scales, e.g., seasonally-interannually [5]. Furthermore, T_a and VPD determined the stomatal conductance and, as a result, they were considered the most important driving force for nighttime water loss [15,26], while SMC is most directly linked with plant transpiration [32,33], particularly in an urban thermal environment. Although the controls of Q_n have been documented for quite a few plant species from different domains [9,17,23], the Q_n regulating mechanisms are not fully understood in a subtropical urban environment. Roth reported that less than 20% of studies are from the subtropical areas concerning the documented research for all the urban climates [34]. Therefore, it is essential to investigate the environmental controls of Q_n across multiple timescales to assess and predict how urban trees respond to and adapt to ongoing climate change, especially in subtropical regions.

The Q_n rates and their response to environmental parameters fluctuate among different plant species due to differences in morphological traits, growth conditions, plant functional types, habitats, plant water consumption behaviors, and tree height and crown diameter [35,36]. Likewise, large interspecific variations in Q_n rates were observed among species growing over similar geographic areas [10]. Additionally, the daily transpiration rate of *Robinia pseudoacacia* is three times smaller than *Tilia cordata* [37]. The previous researchers used

different methods to determine in-depth plant water consumption rates, for example, lysimeter, gas analyzer, statistical models, and eddy covariance measurements [15,38–41]. However, the measurement requirements for these methods are difficult in urban areas concerning the large heterogeneous microclimate, and the approaches might not accurately determine the real conditions [24,42]. The sap flow measurement approach has been considered more reliable for continuously and directly monitoring the whole tree water fluxes in situ [43,44]. Investigations on sap flow rates in trees of urban surroundings are valuable not only to enhance our comprehension of the physiological responses of trees to their hydrometeorological environment but also could help to acknowledge the procedure of water consumption, as well as provide direction to determine the tradeoffs between water supply and demand [24,45].

Shenzhen, a fast developing and densely populated subtropical megacity in South China, has recently faced serious UHI problems with rapid urbanization [46]. In efforts to battle the UHI effect and improve the ecological environment in the area, urban vegetation coverage has been increased. However, the sustainability of many tree species in the region is predicted to be challenged by increasing temperatures and associated irregularities in precipitation with ongoing climate change [45]. Therefore, in this study, we investigated the nighttime sap flow of *Ficus concinna*, a native tree species, over the growing season of seven consecutive years, spanning from 2014 to 2020 under the urban thermal environment. The *F. concinna* trees are commonly used for the greening of subtropical cities. Its plays a vital role in improving the ecological environment and mitigating UHI due to its higher transpiration rate, strong wind and high-temperature resistance, strong shade, large crown structure, and low soil requirements [24,47]. Our objectives of this investigation were to: (1) examine the occurrence and magnitude of Q_n and water-consumption strategies of *F. concinna*; (2) detect the major environmental parameters affecting nighttime sap flow at multiple timescales, and (3) quantify the contribution ratio of Q_n to the overall 24 h sap flow over the entire study period.

2. Materials and Methods

2.1. Site Descriptions and Tree Species

This study was carried out at the campus of Peking University, Shenzhen Graduate School (PUSGS; 22°26′59″–22°51′49″ N, 113°45′44″–114°37′21″ E, ~17 m above mean sea level), in Shenzhen megacity, Guangdong province, southern China. Shenzhen is a coastal megacity that took about 40 years to develop from a small village, with a permanent population of around 13.44 million at the end of 2019. The site has a predominant subtropical humid climate, mainly affected by the South Asian monsoon and thus characterized by a pronounced wet season (May to October) and dry season (November to April). Generally, episodic precipitation events with large intra- and interannual fluctuations are common. Based on long-term meteorological data from the closest Xili Weather Station ~4.5 km from the PUSGS, the mean annual rainfall is approximately 1924.7 mm, on average 75% of which occurs in the growing seasons of each year [24]. The annual mean temperature is 23.3 °C, with the lowest monthly mean T_a (i.e., 14.9 °C) occurring over the coldest month (January) and the highest (i.e., 28.6 °C) during the hottest month (July). The tropical cyclone affects the region about 4–5 times every year. The soils are dominated by brown loamy soil, where the SMC varied mainly in the uppermost part of the soil complex entirely by evapotranspiration and the infiltration of meteoric rainwater. Approximately 50% of this site is covered by vegetation, including shrubs, lawns, and trees [48]. The major tree species growing at the site are *F. concinna*, *Terminalia mantaly*, *Michelia alba*, *Ficus altissima*, *Khaya senegalensis*, *Delonix regia*, *Zoysia matrella*, and *Ficus religiosa*. Measurements were made on 10 trees of *F. concinna* of different ages in the current study. It is a fast-growing tree with a developed root system and a profusion of leathery leaves [49]. For the targeted trees, the height ranged between ~8 and 10 m, with the mean crown area and diameter at breast height (DBH) being 27 ± 1.84 m^2 and 22 ± 2.37 cm (± standard deviation), respectively. The sample trees were randomly selected, representing the study site's DBH class distribution, and were in good condition.

2.2. Sap Flow and Transpiration Measurements

We used manual Granier thermal dissipation probes (TDPs, Ecomatik, Munich, Germany) to continuously assess sap flux density (F_d) of *F. concinna* tree species for 24-h every day over the growing seasons (i.e., May–October) for seven consecutive years (i.e., 2014–2020) [50]. These sap flow measurement sensors (type SF-G) contained a pair of stainless-steel probes (20-mm-long, 2-mm-diameter) inserted at a depth of 20 mm at 90° angles into the stem's sapwood. The sensors were fixed about 1.3 m above the ground after removing the targeted trees' dead tissues and rough bark. In addition, to minimize the thermal effect caused by direct solar radiation, the sensors were attached to the Northside of the trees. All probes were wrapped with transparent plastic and aluminum foil to reduce the influence of light, rainwater, and externally-induced temperature inclines [51,52]. The upper probe was heated with a continuous, direct current (DC, 120 mA) of the heating power of 0.2 W, while the lower probe was unheated and installed about 10 cm beneath the upper one to avoid thermal interference [24]. Furthermore, the sensors were replaced with new ones for more accurate data observation by the start of the growing season over each year. The temperature difference (ΔT, °C) between the probes (i.e., upper and lower sensors) was recorded once every minute and then stored as 10-min averages in a Campbell CR1000-dataloggers (Campbell Scientific, Inc., Logan, UT, USA). These temperature differences were subsequently converted to sap flux densities (F_d, g m^{-2} s^{-1}) by Granier [50], based on a commonly-used equation:

$$F_d = 119 \left(\frac{\Delta Tm - \Delta T}{\Delta T} \right)^{1.231} \quad (1)$$

where ΔT_m is the estimation of maximum ΔT under zero sap flow conditions. To evade the undervaluation of nocturnal sap flux, ΔT_m was determined separately for each tree over 7–10 days during the observation period [53]. Accordingly, ΔT_m was defined when nighttime VPD < 0.05 kPa. Likewise, F_d was calculated using the baseliner program (version 3.0.11, Hydro-Ecology Group, Duke University) [54]. Although this equation can measure absolute water use, it is not affecting the Q_n response to environmental factors.

Daily sap flow (Q, kg d^{-1}) was calculated as reported by Chen et al. with the following equation [9]:

$$Q = F_d \times A_s \times \frac{3600}{1000} \times 24 \quad (2)$$

where A_s is the sapwood area (m^2), and 3600/1000 × 24 is the unit conversion factor to hourly and then daily values. The sapwood area was obtained for 10–12 trees close to the trees observed for the sap flow measurements by using the Haglof increment corer to drill out a wood core at the breast height of the trunks. The width of the sapwood was measured by the different coloration changes between the heartwood and sapwood after dyeing. Subsequently, the relationship between the A_s and the DBH was established based on:

$$A_s = a \times DBH^b \quad (3)$$

where a and b denote the coefficients from the other trees of *F. concinna*, obtained by nonlinear regression analysis (specifically a = 1.01, b = 1.79 in this study). The DBH ranged between 4.8 and 24.5 cm for these trees. We calculated the whole tree transpiration, i.e., water use (T, in mm h^{-1} or d^{-1}) as follows [41]:

$$T = F_d \times \frac{As}{Ac} \times \frac{3600}{1000} \times 24 \quad (4)$$

where A_c is the crown area (m^2). The detailed descriptions of A_c calculation can be found in Hayat et al. [24]. Previous studies have shown that transpiration (T) could also be calculated by the product of canopy conductance and water vapor pressure deficit [26,55,56], with the ratio (i.e., T/VPD) being a proxy for canopy conductance.

2.3. Hydrometeorological Parameters

Micro-hydrometeorological measurements together with the sap flow estimations, were taken from the pre-installed Bowen ratio (BR) tower with an exhibition of sensors located in the experimental area for the same period. The parameters such as T_a (in °C; 225–050YA, Novalynx, Grass Valley, CA, USA), RH (in %), and W_s (in m s^{-1}; 200-WS-02, Novalynx, Grass Valley, CA, USA) were measured at heights of 2, 1.5 and 2 m, respectively, above the ground level. The sensor resolutions for T_a, RH and W_s were ±0.6 °C, ±3% and ±0.2 m s^{-1}, respectively. To characterize the atmospheric demand of water, VPD (in kPa) was subsequently calculated based on recorded T_a and RH [57]. The tipping bucket raingauge (7852M-AB, Davis, CA, USA) was used to record the rainfall amounts (in mm), installed in an opening close to the representative area. The SMCs (in %) were monitored using time-domain reflectometry probes (SM300, Delta-T Devices Ltd., Burwell, Cambridge, UK) at four depths of the soil layer (i.e., 10, 30, 40, and 50 cm) next to the BR system tower. In the present analysis, we used the average values of SMC measured at these four soil depths. All of these micro-hydrometeorological parameters were averaged or summed every 10-min from 60-s over the entire observation period and archived on a CR1000-datalogger (Campbell Scientific, Logan, UT, USA).

2.4. Date Treatment and Gap-Filling

Nighttime and daytime sap flow (i.e., Q_n and Q_d) were characterized as the average sap flow rate from 20:00 to 05:00 and 06:00 to 19:00 local standard time (LST) [5,58]. The current study defined the entire growing season length as the duration ranging from 1 May to 31 October across seven years, except for 2014, which started on 15 July. Similarly, we divided the time of the year, i.e., May as fast growth, June–August as middle growth, and September–October as terminal growth stages of the plants, following Chu et al. [59].

The sap flux measurements were regularly screened and checked to acquire the quality of extracted data based on key principles, i.e., the influence of weather (e.g., cyclone, rainfall, and dewdrops on sensor), instrument failure, out of range fluxes, and atmospheric stability [60]. Missing rainfall data were fulfilled from the daily rainfall measured at the Xili Meteorological Station close to the site. Furthermore, for the missing data in other selected micro-hydrometeorological parameters, the small data gaps (e.g., <2 h in duration) were filled via linear interpolation, whereas longer gaps were filled using the mean diurnal variation approach (MDV) by referring to Falge et al. [61].

2.5. Statistical Analysis

To analyze the potential effects of micro-hydrometeorological variables (e.g., T_a, VPD, RH, W_s, P, SMC, and T/VPD) on Q_n, linear and nonlinear regressions were conducted at multiple temporal scales (i.e., nocturnal-interannual). For the comparison of temporal variations, the data were accumulated to daily nighttime values (Figure 1). We used regression slopes as evidence of Q_n total sensitivity to the various selected site parameters. To test the statistical significance between Q_n and Q_d rates, the one-way ANOVA (analysis of variance) was used at 0.05 critical probability (i.e., αcrit). In addition, the F-statistic was also applied to investigate the significance of the numerous regressions achieved between Q_n and environmental parameters (also, with an $\alpha_{crit} = 0.05$). The percentage of nighttime to the total 24-h sap flow (i.e., $Q_n/Q_{24\text{-}h} \times 100\%$) was calculated for the growing seasons across seven years. The coefficient of variation (i.e., CV) of a parameter was determined as the proportion of its standard deviation (SD) to its mean. All statistical analyses were conducted within a software package such as Excel 2016 (Microsoft Corporation, Redmond, WA, USA) for descriptive statistics and percentile, SPSS (ver.17.0; SPSS Inc., Chicago, IL, USA) for one-way ANOVA and F-statistic, AMOS (ver.17.0; SPSS Inc.) for path analysis, and MATLAB (ver. R2017a, MathWorks Inc., Chicago, IL, USA) for regression analysis, data binning and plots.

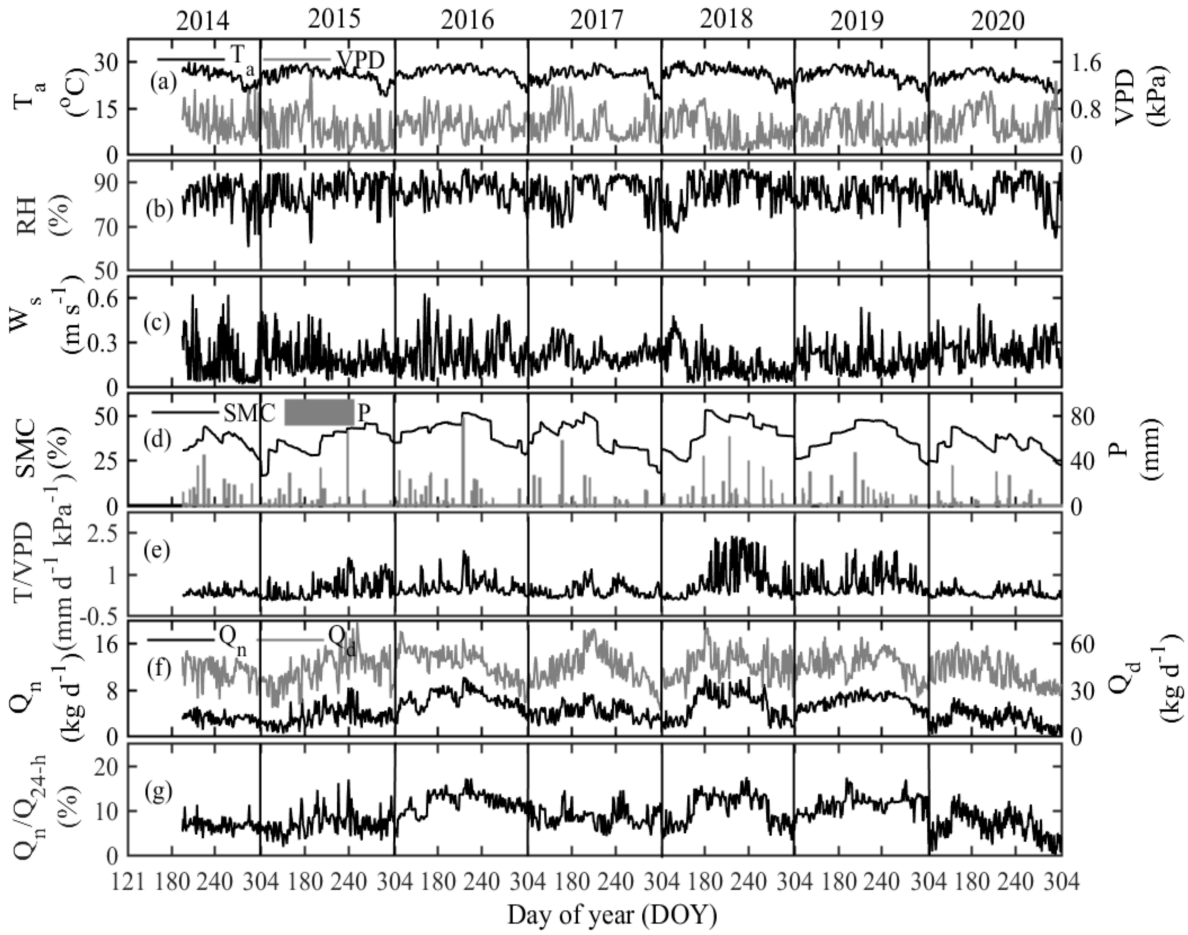


Figure 1. Temporal variations in nighttime mean (**a**) air temperature (T_a), vapor pressure deficit (VPD), (**b**) relative humidity (RH), (**c**) wind speed (W_s), (**d**) soil moisture content (SMC), total nighttime precipitation (P), (**e**) canopy conductance (as indicated by T/VPD), (**f**), nighttime (20:00–05:00), and daytime (06:00–19:00) sap flow rates (Q_n and Q_d, respectively), and (**g**) fraction of nighttime to total 24-h sap flow ($Q_n/Q_{24\text{-}h} \times 100$) during the growing seasons (1 May–31 October) of 2014–2020. The values of SMC are the means of measurements at different depths of 10, 30, 40, and 50 cm over the study site. Note: the data from 1 May to 14 July are missing for 2014.

A path coefficient model was developed to elucidate and determine the direct and indirect regulating mechanisms of micro-hydrometeorological parameters on Q_n. The coefficients of direct paths between two parameters exhibit the standardized partial-regression, whereas indirect pathways designate the product of possible path coefficients, which are summed across all indirect tracks. Furthermore, the sum of the direct and indirect coefficients is the total path coefficient [62,63]. The value of a path coefficient fluctuates from −1.0 to 1.0, representing negative or positive causality. The standardized path coefficient and the discrepancy were estimated by using standardized data on the basis of the maximum likelihood method. To derive the final path diagram, all statistically insignificant paths (e.g., $p > 0.05$) were removed, and coefficients were re-assessed [64].

3. Results

3.1. Variations in Hydrometeorological Parameters

Figure 1a–e shows the daily mean nighttime variations in major hydrometeorological parameters during the observation period of the growing season (1 May–31 October) over seven years. The nighttime T_a, VPD, RH, and W_s were (mean ± standard deviation) 25.68 ± 2.31 °C, 0.48 ± 0.24 kPa, 85.45 ± 6.52%, and 0.194 ± 0.10 m s^{-1}, respectively, during

2014–2020 (Figure 1a–c). The range of T_a, VPD, RH, and W_s across the seven years was 16.51–30.42 °C, 0.03–1.39 kPa, 60.29–96.24%, and 0.01–0.63 m s^{-1}, respectively. During the study period, the interannual monthly mean nighttime T_a had its maximum values in July (27.17 °C), VPD in June (0.66 kPa), RH in September (88.44%), and W_s in May (0.226 m s^{-1}), respectively (Table 1). The growing season annual mean of T_a, VPD, RH, and W_s varied, i.e., 24.73–26.57 °C, 0.41–0.55 kPa, 84.39–86.25%, and 0.15–0.24 m s^{-1}, respectively.

Table 1. Seasonal and interannual variation in nighttime micro-hydrometeorological parameters, sap flow (Q_n) and the ratio of nighttime to 24-h sap flow aggregation ($Q_n/Q_{24\text{-}h} \times 100$) over the growing season (1 May–31 October) of the 2014–2020 observation period. In the table, "CV" and "NA" stand for coefficient of variation and not available, respectively.

Variables	Year	May	Jun	Jul	Aug	Sep	Oct	Average or Sum	CV
T_a (°C)	2014	NA	NA	27.04	26.59	25.21	22.08	25.23	8.87
	2015	25.64	27.63	26.96	26.20	25.45	22.21	25.68	7.34
	2016	25.55	27.57	27.86	27.55	26.67	24.22	26.57	5.37
	2017	23.89	26.84	26.20	27.08	25.88	22.80	25.45	6.75
	2018	27.12	27.22	27.71	27.18	26.20	22.51	26.32	7.33
	2019	25.59	27.47	27.40	26.91	24.64	22.64	25.78	7.35
	2020	24.25	26.18	27.00	24.85	24.57	21.56	24.73	7.57
	Mean	25.34	27.15	27.17	26.62	25.52	22.57	25.68	
VPD (kPa)	2014	NA	NA	0.60	0.57	0.42	0.47	0.52	16.13
	2015	0.43	0.62	0.54	0.37	0.33	0.26	0.42	31.11
	2016	0.50	0.58	0.52	0.44	0.48	0.53	0.51	9.57
	2017	0.47	0.80	0.36	0.49	0.30	0.50	0.49	35.36
	2018	0.41	0.73	0.40	0.32	0.28	0.32	0.41	39.14
	2019	0.49	0.58	0.46	0.42	0.31	0.35	0.43	21.84
	2020	0.46	0.63	0.81	0.41	0.36	0.62	0.55	30.53
	Mean	0.46	0.66	0.53	0.43	0.36	0.44	0.48	
RH (%)	2014	NA	NA	83.83	84.64	87.22	81.85	84.39	2.63
	2015	84.21	82.35	83.79	88.40	88.21	87.90	85.81	3.10
	2016	84.72	85.30	86.80	89.65	87.12	83.89	86.25	2.40
	2017	84.93	78.52	87.03	89.99	91.10	82.74	85.72	5.47
	2018	82.73	84.23	87.11	89.84	88.26	83.48	85.94	3.34
	2019	85.03	81.89	84.39	85.81	86.89	83.99	84.67	2.02
	2020	85.64	84.56	80.77	89.75	90.59	80.93	85.37	4.91
	Mean	84.54	82.81	85.24	87.88	88.44	83.58	85.45	
W_s (m s^{-1})	2014	NA	NA	0.24	0.14	0.20	0.07	0.16	45.51
	2015	0.25	0.18	0.22	0.15	0.16	0.18	0.19	19.28
	2016	0.17	0.26	0.20	0.17	0.24	0.22	0.21	17.38
	2017	0.17	0.29	0.16	0.19	0.17	0.23	0.20	23.89
	2018	0.29	0.15	0.13	0.12	0.11	0.09	0.15	48.24
	2019	0.21	0.19	0.15	0.19	0.15	0.16	0.18	12.72
	2020	0.24	0.23	0.27	0.20	0.22	0.27	0.24	11.57
	Mean	0.226	0.221	0.200	0.170	0.184	0.180	0.194	
P (mm)	2014	NA	NA	50.70	125.60	72.00	33.30	281.60	14.22
	2015	48.00	52.10	90.50	83.60	32.90	6.80	313.90	9.97
	2016	105.00	104.60	44.10	175.00	16.50	34.20	479.40	12.40
	2017	60.00	97.90	103.10	16.50	29.40	31.00	337.90	10.97
	2018	19.78	100.21	39.51	184.15	72.82	14.10	430.57	14.87
	2019	79.60	51.20	69.40	101.20	37.60	33.80	372.80	7.00
	2020	29.98	57.00	14.40	97.40	44.80	8.80	252.38	12.91
	Mean	57.06	77.16	58.81	111.92	43.71	23.14	352.65	

Table 1. *Cont.*

Variables	Year	May	Jun	Jul	Aug	Sep	Oct	Average or Sum	CV
SMC (%)	2014	NA	NA	33.29	39.02	38.33	31.24	35.47	10.71
	2015	27.69	32.13	31.62	40.53	43.57	40.10	35.94	17.49
	2016	39.23	43.02	45.30	49.78	39.27	32.02	41.44	14.69
	2017	40.56	42.86	47.56	33.54	32.18	25.12	36.97	22.13
	2018	28.24	34.15	49.72	49.04	44.57	39.56	40.88	20.90
	2019	32.69	35.16	42.13	45.98	40.52	30.50	37.83	15.83
	2020	29.90	40.91	33.78	37.36	33.88	27.37	33.87	14.45
	Mean	33.05	38.04	40.49	42.18	38.90	32.27	37.48	
T/VPD (mm d^{-1} kPa^{-1})	2014	NA	NA	0.29	0.31	0.35	0.32	0.32	7.03
	2015	0.24	0.19	0.36	0.62	0.57	0.67	0.44	45.85
	2016	0.38	0.47	0.54	0.82	0.55	0.40	0.53	30.16
	2017	0.31	0.21	0.60	0.33	0.51	0.27	0.37	40.61
	2018	0.14	0.44	0.97	1.44	0.97	0.44	0.73	64.74
	2019	0.58	0.47	0.68	0.81	0.90	0.58	0.67	23.59
	2020	0.29	0.36	0.19	0.39	0.39	0.19	0.30	30.02
	Mean	0.32	0.35	0.52	0.67	0.61	0.41	0.48	
Q_n (kg d^{-1})	2014	NA	NA	3.47	3.15	2.78	2.69	3.02	11.87
	2015	1.74	2.59	3.79	4.37	3.94	3.16	3.27	29.75
	2016	5.36	6.08	7.09	8.16	6.13	4.99	6.30	18.44
	2017	3.59	4.31	5.27	4.07	4.11	2.99	4.05	18.76
	2018	2.41	5.76	6.88	7.62	5.60	3.07	5.22	39.65
	2019	4.65	5.76	6.78	6.87	6.83	4.91	5.97	16.93
	2020	1.95	4.62	3.04	3.49	2.74	1.40	2.87	40.56
	Mean	3.28	4.85	5.19	5.39	4.59	3.32	4.39	
$Q_n/Q_{24\text{-}h}$ (%)	2014	NA	NA	7.07	6.64	6.42	6.60	6.68	4.14
	2015	5.39	6.32	7.99	8.40	7.01	7.20	7.05	15.54
	2016	9.13	11.03	12.96	14.04	12.25	10.95	11.73	14.76
	2017	8.58	8.88	8.57	7.35	8.91	8.32	8.43	6.79
	2018	6.40	11.07	12.41	13.34	11.36	6.96	10.26	28.16
	2019	8.99	10.93	12.72	11.64	12.05	12.05	11.40	11.55
	2020	5.09	7.96	7.99	8.80	6.31	3.09	6.54	32.95
	Mean	7.26	9.36	9.96	10.03	9.19	7.88	8.87	

The study site had ample nighttime rainfall during the growing season, with the maximum falling in the month of August (31.37% of the total) and the lowest in October (6.5% of the total) for 2014–2020 (Figure 1d, Table 1). Unusually, in the year of 2016, one large nighttime rainfall event occurred on DOY (day of the year) 215, contributing 77.8 mm of rain, which accounted for 16.2% of the growing season precipitation of that year. Growing season nighttime rainfall summed to 2468.55 mm over seven years, ranging between 252.38 and 479.40 mm, yielding a mean of 352.65 ± 80 mm with a CV of 22.68%. In 2020, minimal amounts of rainfall were observed to be 252.38 mm, about 28.4% lower than the average rainfall amounts (352.65) received in the seven years.

The nighttime SMC varied significantly from season to season, similarly increased in response to rainfall events, and gradually decreased afterward across the seven years (Figure 1d). The daily nighttime SMC, averaged from the measured depths at 10–50 cm, varied from 16.56 to 52.72% for 2014–2020. The high episodes of SMC were evident in the month of August, with the mean value of 42.18%, and the low values occurring in either May or October being 33.05 and 32.27%, respectively (Table 1). The highest annual mean SMC was observed to occur in 2016 (i.e., 41.44%), and the lowest during 2020 (i.e., 33.87%) among the considered seven-year duration. The nighttime T/VPD ranged from 0.026 to 2.38 mm d^{-1} kPa^{-1}, with the maximum values of 0.77, 1.59, 1.86, 1.19, 2.38, 1.91, 0.87 mm d^{-1} kPa^{-1} in years 2014–2020, respectively (Figure 1e). Similar to SMC, the T/VPD clearly showed seasonal pulse dynamics, generally largest in August with the interannual monthly mean of 0.67 mm d^{-1} kPa^{-1} (Table 1). The low SMC in 2020 caused an

extreme clampdown in T/VPD for that year. The highest nighttime annual mean T/VPD was observed in the wet year of 2018, which was 58% higher than the lowest values that occurred in the dry year of 2020.

3.2. Nocturnal Variation in Sap Flow Rates and Its Regulating Parameters

The mean nocturnal pattern in Q_n is consistent with prevailing nighttime hydrometric conditions (Figure 2a–f), with the mean values ranging from about 0.23 kg h^{-1} in May to 0.53 kg h^{-1} in August over seven years. Depending on the time of the night, Q_n showed a steadily decreasing trend from sunset, i.e., from 20:00 to 04:00 LST, and then a progressively increasing trend was observed soon afterward. Both T_a and VPD displayed clear nocturnal variations and gradually decreased to the minimum values after sunset (Figure 2b,c). At the hourly resolution, T_a remained elevated in the month of July, while VPD in June. In contrast, nocturnal RH showed an increasing trend after sunset (20:00 LST), ranging between 88.06% and 94.53% in September and 79.87% and 85.42% in June (Figure 2d). There was no clear pattern observed in W_s, while T/VPD decreased before 03:00 LST and then began to increase afterward, yielding the highest mean value (i.e., 0.06 mm h^{-1} kPa^{-1}) in August and lowest (i.e., 0.02 mm h^{-1} kPa^{-1}) in May (Figure 2e,f).

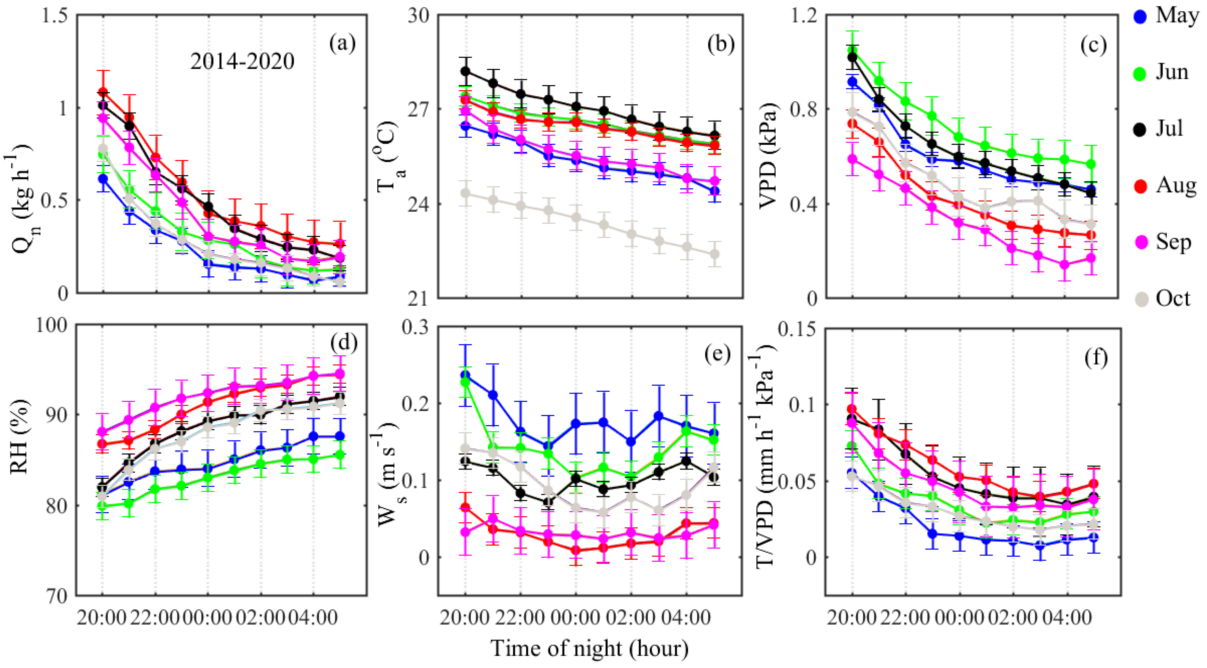


Figure 2. The nocturnal patterns of hourly means of (**a**) sap flow rate (Q_n) and micro-hydrometeorological parameters, including (**b**) air temperature (T_a), (**c**) vapor pressure deficit (VPD), (**d**) relative humidity (RH), (**e**) wind speed (W_s), and (**f**) canopy conductance (as indicated by T/VPD) over the growing seasons of 2014–2020. At a specific time (i.e., 20:00–05:00), each data point shows the mean value for each month, and bars represent the standard error across the 2014–2020 observation period.

At the hourly resolution, Q_n had a significant positive linear correlation and was responsive to fluctuations in T_a, VPD, and T/VPD, whereas it was negatively correlated and was less responsive to RH during the growing seasons of 2014–2020 (Figure 3a–f). The hourly values were bin-averaged at every 0.5 °C, 0.05 kPa, 1.5%, 0.03 m s^{-1}, 0.008 mm h^{-1} kPa^{-1}, and 1% intervals of T_a, VPD, RH, W_s, T/VPD, and SMC, respectively. Nocturnal variation in T_a, VPD, and T/VPD independently explained 63, 70, and 58% of the variation in Q_n, respectively (Figure 3a,b,e). Moreover, Q_n showed no significant linear correlation with W_s and SMC at the hourly resolution (Figure 3d,f).

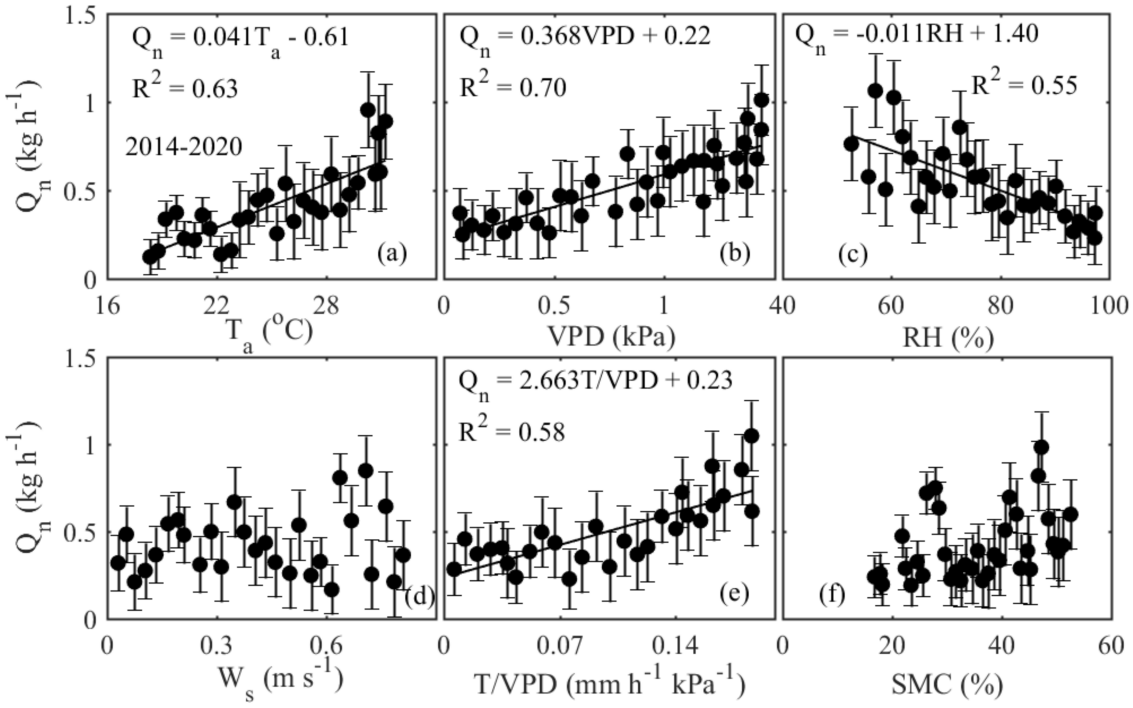


Figure 3. Relationship between nocturnal means of sap flow (Q_n) vs. site micro-hydrometeorological parameters, i.e., (**a**) air temperature (T_a), (**b**) vapor pressure deficit (VPD), (**c**) relative humidity (RH), (**d**) wind speed (W_s), (**e**) canopy conductance (T/VPD), and (**f**) soil moisture content (SMC) during the growing seasons of 2014–2020. Data points represent the binned averages of pooled data from 1 May to 31 October for seven years at every 0.5 °C, 0.05 kPa, 1.5%, 0.03 m s^{-1}, 0.008 mm h^{-1} kPa^{-1}, and 1% intervals of T_a, VPD, RH, W_s, T/VPD, and SMC, respectively. Bars denote standard error.

3.3. Seasonal Variation in Nighttime Sap Flow Rates and Its Regulating Parameters

Daily mean Q_n displayed a pronounced seasonal pattern and tracked the pattern of rainfall and SMC over seven years (Figure 1d,f). Daily Q_n remarkably decreased on rainy days and rapidly increased following the event. The Q_n was much lower than Q_d, ranging from 0.005 to 10.53 kg d^{-1} and 16.66 to 73.54 kg d^{-1}, respectively. The mean difference between Q_n and Q_d was 39.88 ± 7.54 kg d^{-1} with a CV of 18%. The maximum daily Q_n was 5.03, 8.35, 10.14, 7.48, 10.53, 8.35, and 6.65 kg d^{-1} for 2014–2020, respectively. The interannual monthly Q_n was highest in August, yielding a mean value of 5.39 kg d^{-1}, and lowest in May with a mean value of 3.28 kg d^{-1} (Table 1). The annual mean Q_n varied over the growing season with corresponding hydrometeorological parameters, peaked in the middle growth seasons with its values changing from 3.26 (in 2014) to 7.12 kg d^{-1} (in 2016) and then gradually declined during the terminal growth period (Figure 4a–g). The nighttime to daily sap flow ($Q_n/Q_{24\text{-}h}$) ratio showed obvious day-to-day variation, ranging between 0.18% and 17.39% (Figure 1g). The $Q_n/Q_{24\text{-}h}$ had a higher value in August with an interannual monthly mean of 10.03% and lower values in the month of May and October being 7.26 and 7.88%, respectively (Table 1). The $Q_n/Q_{24\text{-}h}$ exhibited a similar seasonal pattern with Q_n over seven years, reaching its maximum in the middle growth period with the mean values ranging between 6.79% and 12.70%, followed by the terminal growth period (Figure 4h).

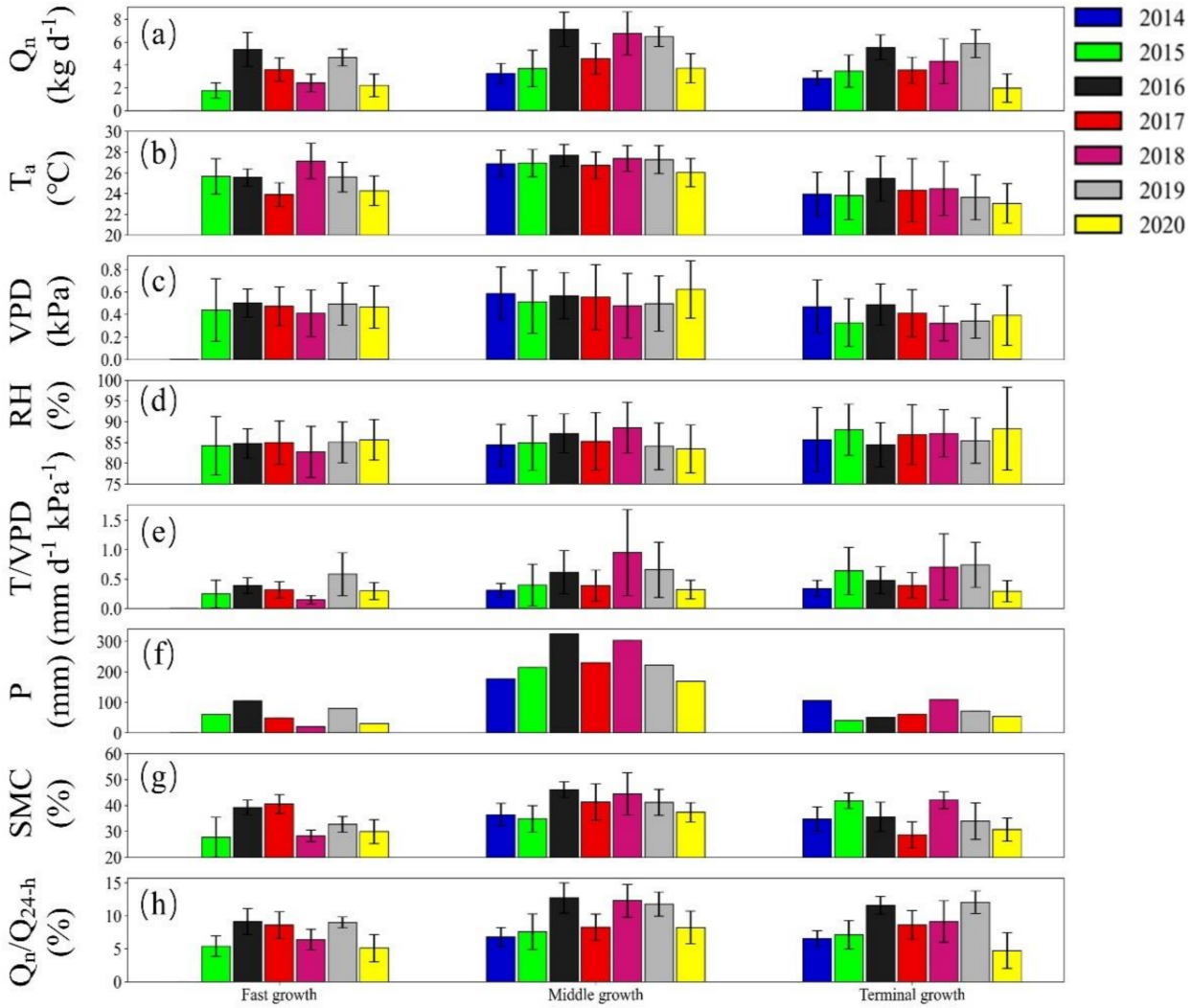


Figure 4. Seasonal courses of nighttime mean (**a**) sap flow rate (Q_n), (**b**) air temperature (T_a), (**c**) vapor pressure deficit (VPD), (**d**) relative humidity (RH), (**e**) canopy conductance (T/VPD), (**f**) total nighttime precipitation (P), (**g**) soil moisture content (SMC), and (**h**) proportion of nighttime sap flow to total 24-h sap flow ($Q_n/Q_{24\text{-h}} \times 100$) at each of three growing periods (i.e., fast growth, middle growth, and terminal growth) over 2014–2020. The data bars are the annual mean values for all parameters, except for the annual total for P at each growing stage. Note: (n = 6 for fast growth period, and n = 7 for middle and terminal growth periods).

The on-site environmental regulating parameters of seasonal variation in Q_n differed among growth stages (Figure 5a–f). At the fast growth stage, an important regulating parameter was VPD, explaining 66% of Q_n variability. During the middle growth stage, the regulating parameters were T_a, T/VPD, P, and SMC, which independently explained 62, 75, 74, and 83% of Q_n variability, respectively, across the seven years. Furthermore, seasonal variation in RH explained 51% of Q_n variability during the terminal growth stage.

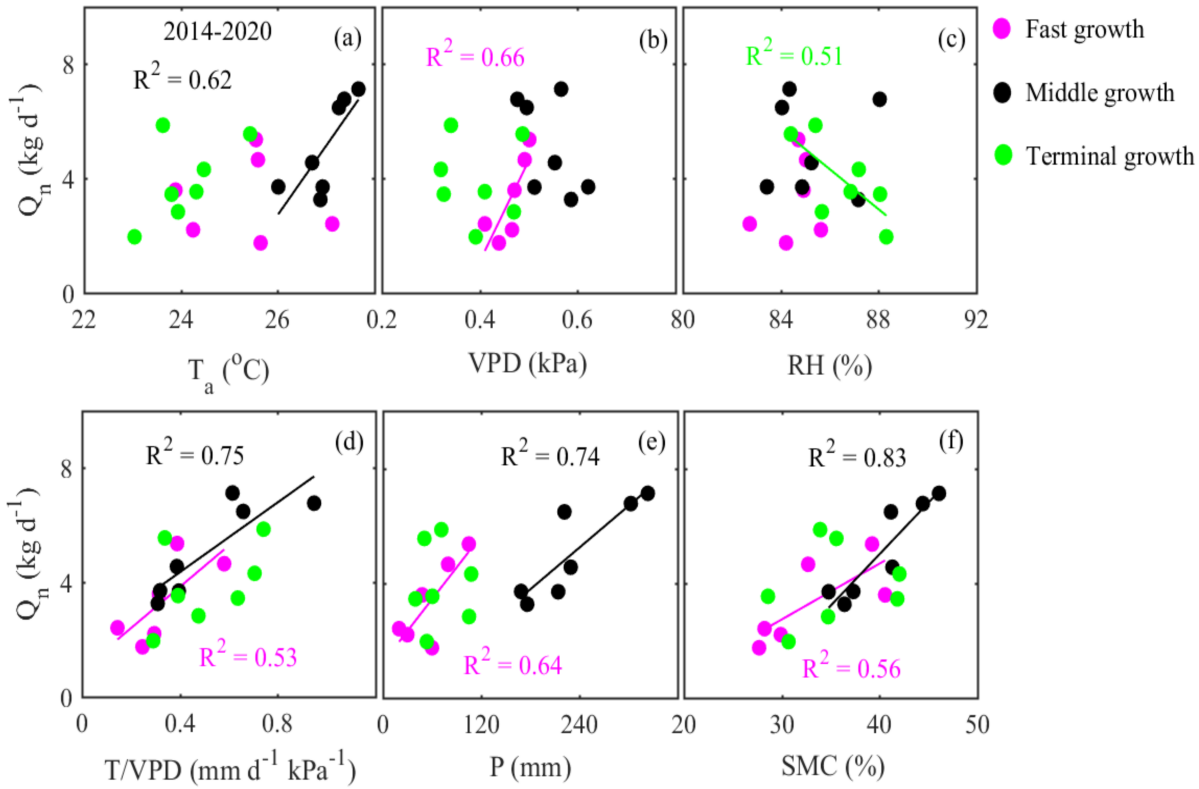


Figure 5. Mean nighttime sap flow (Q_n) at each of the three growing stages (i.e., fast growth, May; middle growth, June–August; and terminal growth, September–October) over 2014–2020 as a function of corresponding selected main explanatory micro-hydrometeorological parameters, including (**a**) air temperature (T_a), (**b**) vapor pressure deficit (VPD), (**c**) relative humidity (RH), (**d**) canopy conductance (T/VPD), (**e**) total nighttime precipitation (P), and (**f**) soil moisture content (SMC). The data points are the annual mean, with the exception of the annual total for P at each growing period, and the given solid lines are statistically significant ($p < 0.05$). Note: (n = 6 for fast growth period, and n = 7 for middle and terminal growth periods).

3.4. Interannual Variation in Nighttime Sap Flow Rates and Its Regulating Parameters

Across the seven consecutive growing seasons, there were significant differences in Q_n corresponding to prevailing nighttime hydrometeorological parameters (i.e., T_a, VPD, RH, W_s, T/VPD, P, and SMC) with an interannual mean of 4.39 ± 1.43 kg d^{-1} and CV of 32.72% (Figure 6a–h, Table 1). Large values of Q_n were observed during wet years, i.e., 2016, 2018, and 2019 with an annual mean of 6.30, 5.22, and 5.97 kg $d^{-1,}$ and low values occurred during dry years, i.e., 2014, 2015, 2017, and 2020 being 3.02, 3.27, 4.05, and 2.87 kg d^{-1}, respectively. The growing season annual mean Q_n significantly contributed to the total 24 h sap flow rate during 2014–2020 by 6.68, 7.05, 11.73, 8.43, 10.26, 11.40, 6.54%, respectively, with an interannual mean ratio of 8.87 ± 2.24% (Figure 6i, Table 1).

Figure 7a–g illustrates the pairwise linear relationships between annual mean Q_n and the corresponding hydrometeorological variables over the growing seasons of 2014–2020. Annual mean Q_n increased with increasing T_a, T/VPD, P, and SMC, with the parameters individually explaining 69, 63, 83, and 76% of the variability in Q_n, respectively (Figure 7a,e–g; with *p*-values, all <0.05). The annual mean Q_n had a tight, positive correlation with P and SMC among these parameters, with the goodness-of-fit being strongest, i.e., 83 and 76%, respectively. In contrast, the effects of VPD, RH, and W_s on annual mean Q_n were weak and statistically insignificant (Figure 7b–d; $p > 0.05$). Furthermore, path analysis demonstrated that the dynamics of annual mean Q_n were mainly regulated by T_a, T/VPD, P, and SMC with direct path coefficients of 0.58, 0.55, 0.73, and 0.62, respectively (Figure 8). As mediated by

T/VPD and SMC, the indirect path coefficients through separate pathways of T_a and P on Q_n were 0.18 and 0.24, respectively. W_s significantly enhanced VPD, yielding a path coefficient of 0.61, but had no discernible direct effect on Q_n. The indirect path coefficients of VPD and W_s on Q_n (i.e., −0.29 and −0.18) are equivalent to the total path coefficients.

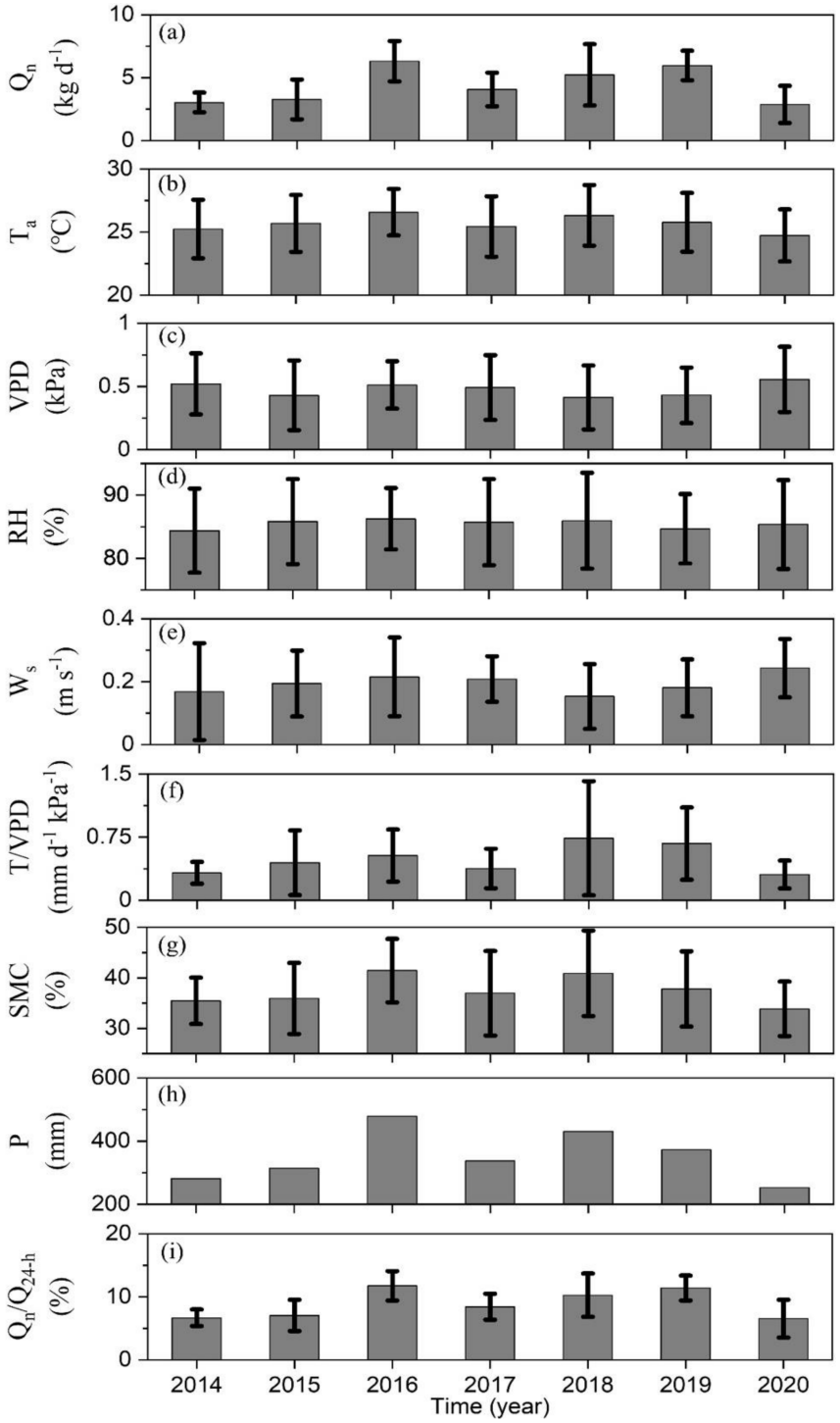


Figure 6. Interannual courses in nighttime growing season annual means of (**a**) sap flow rate (Q_n), (**b**) air temperature (T_a), (**c**) vapor pressure deficit (VPD), (**d**) relative humidity (RH), (**e**) wind speed (W_s), (**f**) canopy conductance (T/VPD), (**g**) soil moisture content (SMC), (**h**) total nighttime precipitation (P), and (**i**) ratio of nighttime sap flow to total 24-h sap flow ($Q_n/Q_{24\text{-}h} \times 100$) during 2014–2020. Error bars are given for annual mean of all the selected variables except total precipitation.

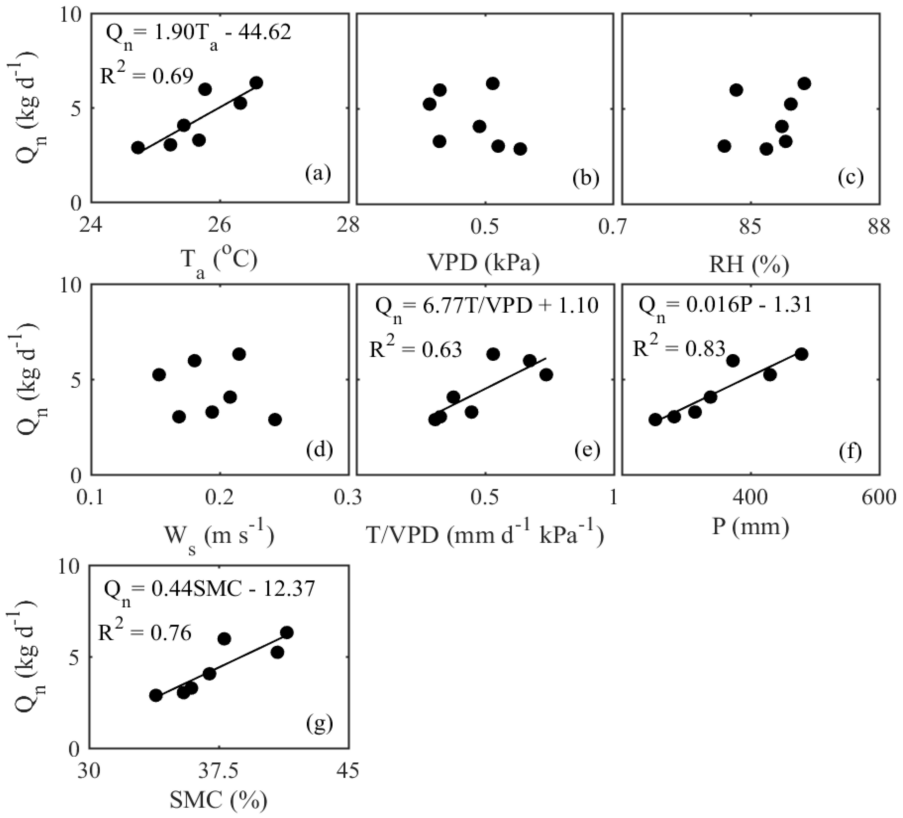


Figure 7. Interannual response of growing season nighttime mean sap flow (Q_n) to site micro-hydrometeorological parameters, i.e., (**a**) air temperature (T_a), (**b**) vapor pressure deficit (VPD), (**c**) relative humidity (RH), (**d**) wind speed (W_s), (**e**) canopy conductance (T/VPD), (**f**) soil moisture content (SMC), and (**g**) total nighttime precipitation (P) over 2014–2020. Data points indicate growing season annual nighttime means for all parameters but annual total for P.

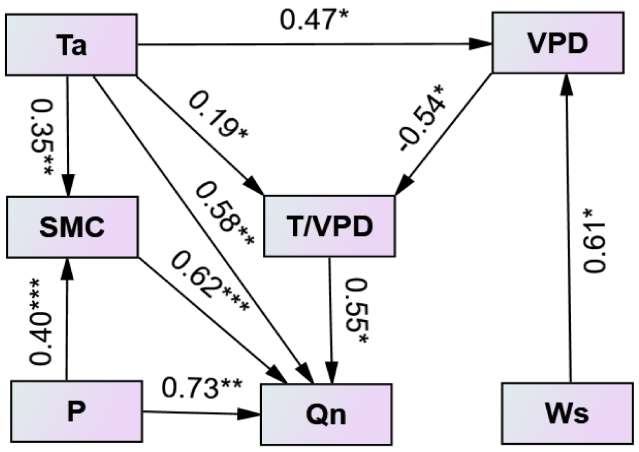


Figure 8. Direct and indirect effects of nighttime micro-hydrometeorological parameters, including air temperature (T_a), vapor pressure deficit (VPD), wind speed (W_s), canopy conductance (T/VPD), soil moisture content (SMC), and total nighttime precipitation (P) on interannual variation in nighttime sap flow (Q_n). Standardized path coefficients (i.e., −1 to 1) are given for each arrow, where negative and positive effects are indicated by negative and positive values, respectively. Asterisks one, two and three (i.e., "*", "**" and "***") stand for significance levels < 0.05, 0.01 and 0.001, respectively. Data used were the growing season annual nighttime means for all parameters, but annual total for P from 2014–2020.

4. Discussion

4.1. Environmental Control on Sap Flow Rates at the Hourly/Nocturnal Scale

Several prior researchers have suggested the possible causes and significance of the wide occurrence of nocturnal sap flow (transpiration), such as transferring carbohydrates [16], promoting nutrient acquisition [65], and advanced opening of stomata in the early morning [13]. However, the robust understanding of nighttime sap flow significance and physiological basis remains unexplained [20,23,66], particularly at multiple timescales. We installed one commercial sap flow sensor for each tree because we assumed no azimuthal variability in the sap flow for the current study. In addition, the need for tree protection and the required number of instruments also limited the use of more sap flow sensors. Our results showed that the Q_n rate was relatively more stable during nighttime than the Q_d rate during daytime (Figure 1f) and varied with changes in micro-hydrometeorological parameters, which is consistent with previous studies [4,31]. The Q_n rate decrease after sunset from May to October may be related to the decreasing trend of T_a and VPD and increasing RH at nighttime before dawn (Figure 2a–d) [5,58,67]. The results show that nocturnal patterns in Q_n and T_a and VPD match during nighttime, supporting that T_a and VPD are Q_n's primary drivers during the night. Moreover, maximum T_a and minimum RH was observed in the early night, whereas minimum T_a and maximum RH were in the early morning. A previous study revealed a better cooling effect of urban vegetation on the thermal environment during nighttime (particularly from 20:00 to 24:00 LST) than during daytime [68], which supports our findings of a higher Q_n rate in the early night. The higher W_s at the beginning of the night (Figure 2e) can contribute to the magnitude and nocturnal variation of VPD and, thus, nocturnal sap flow, which is in line with previous researchers who revealed that higher W_s lead to higher VPD [27,69]. Our results are unified with previous studies, indicating that Q_n has a firm positive relationship with T_a and VPD [8,70], T/VPD [26] and a significant negative correlation with RH at the hourly resolution (Figure 3). The influence of canopy conductance on Q_n can deviate within species and fluctuate in environmental parameters such as T_a, VPD, and SMC over many sites [5,71]. In general, T/VPD has a drastic control on Q_n under scarce soil water availability. However, the parameters, i.e., W_s and SMC elucidated a very small segment of Q_n variability at an hourly resolution because W_s had no clear pattern [67,72], and the temporal variations in SMC were generally very gradual [35].

4.2. Environmental Control on Nighttime Sap Flow Rates at the Seasonal Scale

Mean nighttime sap flow and its seasonal variability with response to variations in micro-hydrometeorological variables fluctuated by plant functional type in a way that is parallel with prior observations [4,5,40] (Figure 1). The seasonal precipitation distribution and associated soil water availability were the most important stimulants in regulating the Q_n rate (Figure 1d,f) and accelerating trees' carbon assimilation. As a result, the response of Q_n was examined to be highest after ample amounts of rainfall, triggering soil water replenishment, which is consistent with previous studies that suggested sap flow should increase with an increase in precipitation [29,45,73]. The Q_n showed a strong dependence on SMC boosted by rainfall during August at the monthly timescales, leading to the large interannual variation in monthly Q_n and T/VPD over the same period (Table 1). Furthermore, the greatest variability in Q_n was observed during the middle growth stage (Figure 4), matching larger variations in T_a and infiltration of meteoric water into the soil during this period [7,74], typically associated with the start of the site monsoon season. Consequently, the conversion from the excessively dry to wet season occurred with the onset of the monsoon season, leading to considerable seasonal variations in most micro-hydrometeorological parameters and plant characteristics [59,75]. This seasonal pattern was found to be consistent with those in many subtropical urban tree species, including *Eucalyptus citriodora*, *Acacia auriculaeformis* and *Schima superba* [45,74].

Previous studies revealed that the proportion of Q_n to total daily sap flow differs significantly based on trees' morphological traits, age [31,76], and contrasting habitats [9]. The

average Q_n accounted for up to 0.18%–17.39% of the $Q_{24\text{-}h}$ aggregate sap flow (Figure 1g), which can affect the water balance and cause disequilibrium between the status of soil water and predawn leaf water potential [8,77]. Therefore, the estimation of nocturnal water use of trees could provide evidence for the selection of suitable plantation species on the basis of their seasonal behavior of nighttime transpiration. However, there is a dearth of studies on the nighttime water use of *F. concinna* in subtropical urban areas; hence, the current study's findings were related to other tree species growing in different biomes. Our results are in line with prior achievements, showing that the seasonal contribution of nocturnal to 24-h sap flow (i.e., 6.79%–12.70%, Figure 4h) during the middle growth stage across seven years fell within the mean $Q_n/Q_{24\text{-}h}$, ranging between 3.0% and 18%, as documented for other ecosystems [4,78,79]. Some other studies carried out on many woody plants reported the fractions for up to 15%–30% over a savanna site [65], 10%–32% in semiarid regions of western USA [18], 10%–30% in Mediterranean holm oak forests [80], and reached to the maximum ratios of 50% in arid to semiarid regions of northwestern Australia [81]. As a result, large proportions point to low water consumption during the daytime and high sap flow at night. The possible reason for substantial water loss during the night through transpiration was demonstrated as the overall high atmospheric water demand, i.e., T_a and VPD.

At seasonal scales, the effect of micro-hydrometeorological forcing on nighttime sap flow has seldom been investigated over subtropical urban plantations [58]. In several other ecosystems, it has been previously revealed that site environmental parameters, including T_a, VPD, and SMC, were generally the most significant variables affecting Q_n [5,8,9,80]. The high VPD reflects the changes in water potential between atmospheric demand and leaves, which influences the canopy conductance, resulting in nighttime water losses [4,82]. Similarly, SMC dynamics were observed to be crucial in defining the timing of the growth rates in plants because water availability is fundamental for increases in both photosynthetic capacity and transpiration rates [59,83–85]. Furthermore, the prior study revealed that water scarcity might change the plant physiology, delay the development of the canopy structure and even cause tree mortality, which underscores the impact of precipitation variability on the existing plantation growth [86]. At our site, the Q_n was strongly correlated and highly responsive to VPD during fast growth, T_a, T/VPD, and P-induced-SMC during middle growth, and RH in the terminal growth stages (Figure 5a–f), because of the pronounced variability in T_a and P-induced-soil water conditions (Figure 4b,f,g). These results are comparable with the findings obtained by previous research, which showed that SMC did not only affect transpiration but also mediated the influences of other micro-hydrometeorological parameters on the sap flow rate [4,9,24,28,58]. Another explanation may be the irrigation practices, i.e., roughly once a week during the dry period (according to the management services office), which support the nighttime plants' water consumption. Therefore, to optimize tree growth development and functioning, irrigation practices during the dry seasons are more productive than irrigation during any other time of the year [24,87]. To further elucidate, the Q_n rate positively increased with increasing T_a and T/VPD under sufficient water availability during the middle growth stage while negatively decreased with high seasonal RH over the terminal growth stage. Additionally, the fluctuations in Q_n rates may deliver ecophysiological improvements to plants via boosting photosynthesis and promoting fast growth [8] and could be adaptive feedback to dry environmental conditions [35].

4.3. Environmental Control on Nighttime Sap Flow Rates at the Interannual Scale

The consecutive seven-year nighttime observation period (i.e., covered wet and dry years) provided an opportunity to investigate Q_n's long-term variations and responses under thermal environmental conditions. The growing season means annual Q_n varied significantly with response to environmental drivers, largely congruent to the rain-fed soil water (Figure 6a–h, Table 1). Typically, over a longer timescale (i.e., interannually), SMC can explain a massive fraction of variability in transpiration because, in a short-time period,

the physical fluctuations in SMC are very moderate [29,67]. In the current study, we found the highest growing season mean annual Q_n in the wet and warm years (i.e., 2016, 2018, and 2019), which is in line with the previous observations that atmospheric water demand increases with higher T_a under an ample soil water environment [45,70,88]. In contrast, during the dry and cold years of 2014, 2015, 2017, and 2020, the T/VPD and Q_n were observed to be low because there was frequent scarce SMC to meet the atmospheric demand for water. Furthermore, over the periods of excessive dryness, the Q_n decreased rapidly, accentuating the water conservation strategy retained by woody plants [23,35]. Similarly, trees can lessen the impacts of higher nighttime water losses through stomatal closure in the dry periods to prevent functional damage to themselves [33,58,72]. The different plant species growing in different habitats with diverging traits lead to species-specific differences in transpiration rate. In our previous research, we found that the daily mean transpiration rate of *F. concinna* ranged from 0.27 to 2.80 mm d^{-1} with a mean value of 1.46 mm d^{-1} [24], which was higher than the transpiration rate of other urban tree species ranging from 0.1 to 0.6 mm d^{-1} [45]. The nighttime water consumption (i.e., transpiration) of *F. concinna* ranged from 0.003 to 0.35 mm per night, with an average of 0.15 mm per night (data not shown). However, the differences can often be related to species-specific hydraulic characteristics and the amount of precipitation received. Our findings are in line with earlier studies, which showed that Q_n could contribute considerably to $Q_{24\text{-}h}$ (Figure 6i, Table 1) [18,21,79]. However, the growing season annual mean proportions were highest in the wet years compared to dry years because the promotion in stomatal aperture and physiological activity in wet conditions causes Q_n to be more sensitive to environmental drivers (i.e., T_a and VPD), while the reduction in stomatal conductance generally leads Q_n to be less responsive to environmental stress conditions [5,17,29]. Previous studies documented that stem refilling may also occur at night, which may be responsible for recharging the depleted water storage of plants primarily caused by daytime transpiration [89,90]. Furthermore, the nighttime sap flow is more elevated before midnight, indicating to fill up the water storage deficit reduced by daytime water consumption [91]. The refilling of the stem water storage deficit could contribute up to 15%–25% of daily sap flow [8]. The basal sap flow starts rising nearly simultaneously with environmental parameters in the morning.

Generally, the regulating mechanism of the hydrometeorological parameters on nighttime sap flow of vegetation growing in an urban thermal environment at interannual scales is quite a new concept. Estimating the relationship between the plant's water use at night with these regulating parameters encourages water management aspects and also improves the understanding of the role of urban design in the water budget [72]. We found that at interannual scales, Q_n was significantly conformed to the regulating parameters of T_a, T/VPD, P, and SMC; however, this connection was shown to be more tightly coupled between Q_n and P-induced changes in SMC (Figure 7a–g). These findings are supported by prior studies which demonstrated that unlike VPD and W_s influencing Q_n at a short timescale [9,23], meteoric water input to soils would be an important regulating parameter of Q_n over a longer timescale [5,35,92] because the temporal variations in soil water are generally very gradual over a short period. The scale issue in the nighttime sap flow response to hydrometeorological parameters is a long-lasting topic [91]. The plants' water consumption differs primarily with atmospheric demand under sufficient water availability. Over short timescales (i.e., hourly/daily), T_a and VPD exert significant control on Q_n by affecting the stomatal conductance. In addition, Chen et al. also anticipated that variations of SMC over the longer term could explain a large level of interannual alterations of transpiration [45]. Path analysis further reinforced these relationships (Figure 8). The parameters T_a, T/VPD, and meteoric water to soil had a direct positive control on Q_n, while VPD and W_s had an indirect control on Q_n by influencing T/VPD and soil water availability. Consequently, this indirect relation counterbalanced the direct control on Q_n. In addition, the influences of VPD and W_s on Q_n are dependent on canopy conductance and soil water conditions [9,62].

5. Conclusions

Magnitude and patterns of nighttime sap flow in urban trees (e.g., *F. concinna*) with the influences of environmental parameters were analyzed at multiple timescales over seven years. The results indicate that predominant nighttime hydrometeorological parameters may cause Q_n to vary from nocturnal to interannual timescales. Variations in T_a, VPD, and T/VPD largely regulated Q_n at the hourly resolutions during the growing seasons. However, regulating parameters of variation in Q_n differed seasonally, with VPD exhibited to be the most important during the fast growth, T_a, T/VPD, and P-induced-SMC during the middle growth, and RH during the terminal growth stages of the trees. During wet years, Q_n was generally higher than in dry years. Interannually, the variability in Q_n was mainly regulated by T_a, T/VPD, P, and SMC. The soil water availability, together with changing environmental parameters across temporal scales, caused Q_n to respond differently, indicating that plants had a physiological capacity to acclimatize to soil dryness. Across the seven years, Q_n was lower than Q_d with a CV of 18%. The significant contribution of Q_n to the 24 h sap flow ranged between 0.18% and 17.39%, suggesting the importance of Q_n to the water status and tree's transpiration-induced cooling in a thermal environment in urban areas. However, further investigation requires evaluating the nighttime transpiration-induced cooling efficiency in the context of increasing the UHI effect (specifically under high nighttime T_a and VPD) with future climate change and urbanization.

Author Contributions: All authors intellectually contributed to this study. M.H.: conceptualization, methodology, writing—original draft. C.Y.: conceptualization, funding acquisition. J.X.: data curation, investigation, B.X.: investigation, data acquisition, L.Q.: visualization, resources, B.W.: investigation, data acquisition, A.K.: validation, writing—review and editing, M.K.: investigation, writing—review and editing, Z.Z.: formal analysis, methodology, G.Q.: supervision, conceptualization, funding acquisition. All authors have read and agreed to the published version of the manuscript.

Funding: The study was supported by grants from Shenzhen Science and Technology Project (GXWD20201231165807007-20200827105738001, JCYJ20180504165440088), the Chinese Ministry of Science and Technology Projects (YS2017YFE0116500, 2017FY100206-03), and the National Natural Science Foundation of China (42001022).

Data Availability Statement: Contact Guo Yu Qiu (qiugy@pkusz.edu.cn) or Chunhua Yan (yanch@pku.edu.cn) to access this research data.

Acknowledgments: We thank Shenglin Tan, Zhenhua Wang, Tong Li, Xiaohui Yu, Chenghaoxian Jiang, and Haiyan Wen for their assistance with field measurements and instrument maintenance.

Conflicts of Interest: The authors declare no conflict of interests.

References

1. Bahn, M.; Reichstein, M.; Guan, K.; Moreno, J.M.; Williams, C. Preface: Climate extremes and biogeochemical cycles in the terrestrial biosphere: Impacts and feedbacks across scales. *Biogeosciences* **2015**, *12*, 4827–4830. [CrossRef]
2. Domec, J.C.; Ogée, J.; Noormets, A.; Jouangy, J.; Gavazzi, M.; Treasure, E.; King, J.S. Interactive effects of nocturnal transpiration and climate change on the root hydraulic redistribution and carbon and water budgets of southern United States pine plantations. *Tree Physiol.* **2012**, *32*, 707–723. [CrossRef] [PubMed]
3. Davy, R.; Esau, I.; Chernokulsky, A.; Outten, S.; Zilitinkevich, S. Diurnal asymmetry to the observed global warming. *Int. J. Climatol.* **2017**, *37*, 79–93. [CrossRef]
4. Siddiq, Z.; Cao, K.F. Nocturnal transpiration in 18 broadleaf timber species under a tropical seasonal climate. *For. Ecol. Manag.* **2018**, *418*, 47–54. [CrossRef]
5. Hayat, M.; Iqbal, S.; Zha, T.; Jia, X.; Qian, D.; Bourque, C.P.A.; Yang, R. Biophysical control on nighttime sap flow in *Salix psammophila* in a semiarid shrubland ecosystem. *Agric. For. Meteorol.* **2021**, *300*, 108329. [CrossRef]
6. Zeppel, M.J.B.; Lewis, J.D.; Phillips, N.G.; Tissue, D.T. Consequences of nocturnal water loss: A synthesis of regulating factors and implications for capacitance, embolism and use in models. *Tree Physiol.* **2014**, *34*, 1047–1055. [CrossRef]
7. Fu, Y.H.; Liu, Y.; De Boeck, H.J.; Menzel, A.; Nijs, I.; Peaucelle, M.; Janssens, I.A. Three times greater weight of daytime than of night-time temperature on leaf unfolding phenology in temperate trees. *New Phytol.* **2016**, *212*, 590–597. [CrossRef]
8. Daley, M.J.; Phillips, N.G. Interspecific variation in nighttime transpiration and stomatal conductance in a mixed New England deciduous forest. *Tree Physiol.* **2006**, *26*, 411–419. [CrossRef]

9. Chen, Z.; Zhang, Z.; Sun, G.; Chen, L.; Xu, H.; Chen, S. Biophysical controls on nocturnal sap flow in plantation forests in a semi-arid region of northern China. *Agric. For. Meteorol.* **2020**, *284*, 107904. [CrossRef]
10. Caird, M.A.; Richards, J.H.; Donovan, L.A. Nighttime stomatal conductance and transpiration in C3 and C4 plants. *Plant Physiol.* **2007**, *143*, 4–10. [CrossRef]
11. Goldstein, G.; Bucci, S.J.; Scholz, F.G. Why do trees adjust water relations and hydraulic architecture in response to nutrient availability? *Tree Physiol.* **2013**, *33*, 238–240. [CrossRef]
12. Gansert, D. Xylem sap flow as a major pathway for oxygen supply to the sapwood of birch (*Betula pubescens* Ehr.). *Plant Cell Environ.* **2003**, *26*, 1803–1814. [CrossRef]
13. Resco de Dios, V.; Loik, M.E.; Smith, R.; Aspinwall, M.J.; Tissue, D.T. Genetic variation in circadian regulation of nocturnal stomatal conductance enhances carbon assimilation and growth. *Plant Cell Environ.* **2016**, *39*, 3–11. [CrossRef]
14. Benyon, R.G. Nighttime water use in an irrigated *Eucalyptus grandis* plantation. *Tree Physiol.* **1999**, *19*, 853–859. [CrossRef]
15. Fisher, J.B.; Baldocchi, D.D.; Misson, L.; Dawson, T.E.; Goldstein, A.H. What the towers don't see at night: Nocturnal sap flow in trees and shrubs at two AmeriFlux sites in California. *Tree Physiol.* **2007**, *27*, 597–610. [CrossRef]
16. Marks, C.O.; Lechowicz, M.J. The ecological and functional correlates of nocturnal transpiration. *Tree Physiol.* **2007**, *27*, 577–584. [CrossRef]
17. Zhao, C.; Si, J.; Feng, Q.; Yu, T.; Li, P.; Forster, M.A. Nighttime transpiration of *Populus euphratica* during different phenophases. *J. For. Res.* **2019**, *30*, 435–444. [CrossRef]
18. Snyder, K.A.; Richards, J.H.; Donovan, L.A. Night-time conductance in C3 and C4 species: Do plants lose water at night? *J. Exp. Bot.* **2003**, *54*, 861–865. [CrossRef]
19. Lombardozzi, D.L.; Zeppel, M.J.; Fisher, R.A.; Tawfik, A. Representing nighttime and minimum conductance in CLM4. 5: Global hydrology and carbon sensitivity analysis using observational constraints. *Geosci. Model Dev.* **2017**, *10*, 321–331. [CrossRef]
20. Dawson, T.E.; Burgess, S.S.; Tu, K.P.; Oliveira, R.S.; Santiago, L.S.; Fisher, J.B.; Ambrose, A.R. Nighttime transpiration in woody plants from contrasting ecosystems. *Tree Physiol.* **2007**, *27*, 561–575. [CrossRef]
21. Forster, M.A. How significant is nocturnal sap flow? *Tree Physiol.* **2014**, *34*, 757–765. [CrossRef]
22. Wallace, J.; McJannet, D. Processes controlling transpiration in the rainforests of north Queensland, Australia. *J. Hydrol.* **2010**, *384*, 107–117. [CrossRef]
23. Rosado, B.H.; Oliveira, R.S.; Joly, C.A.; Aidar, M.P.; Burgess, S.S. Diversity in nighttime transpiration behavior of woody species of the Atlantic Rain Forest, Brazil. *Agric. For. Meteorol.* **2012**, *158*, 13–20. [CrossRef]
24. Hayat, M.; Xiang, J.; Yan, C.; Xiong, B.; Wang, B.; Qin, L.; Qiu, G.Y. Environmental control on transpiration and its cooling effect of *Ficus concinna* in a subtropical city Shenzhen, southern China. *Agric. For. Meteorol.* **2022**, *312*, 108715. [CrossRef]
25. Bosch, D.D.; Marshall, L.K.; Teskey, R. Forest transpiration from sap flux density measurements in a Southeastern Coastal Plain riparian buffer system. *Agric. For. Meteorol.* **2014**, *187*, 72–82. [CrossRef]
26. Resco de Dios, V.; Roy, J.; Ferrio, J.P.; Alday, J.G.; Landais, D.; Milcu, A.; Gessler, A. Processes driving nocturnal transpiration and implications for estimating land evapotranspiration. *Sci. Rep.* **2015**, *5*, 10975. [CrossRef]
27. Rahman, M.A.; Moser, A.; Rötzer, T.; Pauleit, S. Microclimatic differences and their influence on transpirational cooling of *Tilia cordata* in two contrasting street canyons in Munich, Germany. *Agric. For. Meteorol.* **2017**, *232*, 443–456. [CrossRef]
28. Hayat, M.; Zha, T.; Jia, X.; Iqbal, S.; Qian, D.; Bourque, C.P.A.; Yang, R. A multiple-temporal scale analysis of biophysical control of sap flow in *Salix psammophila* growing in a semiarid shrubland ecosystem of northwest China. *Agric. For. Meteorol.* **2020**, *288*, 107985. [CrossRef]
29. Iqbal, S.; Zha, T.; Jia, X.; Hayat, M.; Qian, D.; Bourque, C.P.A.; Khan, A. Interannual variation in sap flow response in three xeric shrub species to periodic drought. *Agric. For. Meteorol.* **2021**, *297*, 108276. [CrossRef]
30. Phillips, N.G.; Lewis, J.D.; Logan, B.A.; Tissue, D.T. Inter-and intra-specific variation in nocturnal water transport in Eucalyptus. *Tree Physiol.* **2010**, *30*, 586–596. [CrossRef]
31. Yu, T.; Feng, Q.; Si, J.; Zhang, X.; Alec, D.; Zhao, C. Evidences and magnitude of nighttime transpiration derived from *Populus euphratica* in the extreme arid region of China. *J. Plant Biol.* **2016**, *59*, 648–657. [CrossRef]
32. Ma, F.; Kang, S.; Li, F.; Zhang, J.; Du, T.; Hu, X.; Wang, M. Effect of water deficit in different growth stages on stem sap flux of greenhouse grown pear-jujube tree. *Agric. Water Manag.* **2007**, *90*, 190–196. [CrossRef]
33. Zha, T.; Qian, D.; Jia, X.; Bai, Y.; Tian, Y.; Bourque, C.P.A.; Peltola, H. Soil moisture control of sap-flow response to biophysical factors in a desert-shrub species, *Artemisia ordosica*. *Biogeosciences* **2017**, *14*, 4533–4544. [CrossRef]
34. Roth, M. Review of urban climate research in (sub) tropical regions. *Int. J. Climatol. J. R. Meteorol. Soc.* **2007**, *27*, 1859–1873. [CrossRef]
35. Fang, W.; Lu, N.; Zhang, Y.; Jiao, L.; Fu, B. Responses of nighttime sap flow to atmospheric and soil dryness and its potential roles for shrubs on the Loess Plateau of China. *J. Plant Ecol.* **2018**, *11*, 717–729. [CrossRef]
36. Rahman, M.A.; Stratopoulos, L.M.; Moser-Reischl, A.; Zölch, T.; Häberle, K.H.; Rötzer, T.; Pauleit, S. Traits of trees for cooling urban heat islands: A meta-analysis. *Build. Environ.* **2020**, *170*, 106606. [CrossRef]
37. Rahman, M.A.; Moser, A.; Gold, A.; Rötzer, T.; Pauleit, S. Vertical air temperature gradients under the shade of two contrasting urban tree species during different types of summer days. *Sci. Total Environ.* **2018**, *633*, 100–111. [CrossRef]
38. Young, M.H.; Wierenga, P.J.; Mancino, C.F. Monitoring near-surface soil water storage in turfgrass using time domain reflectometry and weighing lysimetry. *Soil Sci. Soc. Am. J.* **1997**, *61*, 1138–1146. [CrossRef]

39. Gill, S.E.; Rahman, M.A.; Handley, J.F.; Ennos, A.R. Modelling water stress to urban amenity grass in Manchester UK under climate change and its potential impacts in reducing urban cooling. *Urban For. Urban Green.* **2013**, *12*, 350–358. [CrossRef]
40. Konarska, J.; Uddling, J.; Holmer, B.; Lutz, M.; Lindberg, F.; Pleijel, H.; Thorsson, S. Transpiration of urban trees and its cooling effect in a high latitude city. *Int. J. Biometeorol.* **2016**, *60*, 159–172. [CrossRef]
41. Qiu, G.Y.; Yu, X.; Wen, H.; Yan, C. An advanced approach for measuring the transpiration rate of individual urban trees by the 3D three-temperature model and thermal infrared remote sensing. *J. Hydrol.* **2020**, *587*, 125034. [CrossRef]
42. Goulden, M.L.; Field, C.B. Three methods for monitoring the gas exchange of individual tree canopies: Ventilated-chamber, sap-flow and Penman-Monteith measurements on evergreen oaks. *Funct. Ecol.* **1994**, *8*, 125–135. [CrossRef]
43. Granier, A.; Biron, P.; Breda, N.; Pontailler, J.Y.; Saugier, B. Transpiration of trees and forest stands: Short and long-term monitoring using sapflow methods. *Glob. Change Biol.* **1996**, *2*, 265–274. [CrossRef]
44. Litvak, E.; McCarthy, H.R.; Pataki, D.E. A method for estimating transpiration of irrigated urban trees in California. *Landsc. Urban Plan.* **2017**, *158*, 48–61. [CrossRef]
45. Chen, X.; Zhao, P.; Hu, Y.; Ouyang, L.; Zhu, L.; Ni, G. Canopy transpiration and its cooling effect of three urban tree species in a subtropical city-Guangzhou, China. *Urban For. Urban Green.* **2019**, *43*, 126368. [CrossRef]
46. Zou, Z.; Yan, C.; Yu, L.; Jiang, X.; Ding, J.; Qin, L.; Qiu, G. Impacts of land use/land cover types on interactions between urban heat island effects and heat waves. *Build. Environ.* **2021**, *204*, 108138. [CrossRef]
47. Zhang, Z.; Jiang, D.; Xu, Y.; Xiao, J.; Wang, J.; He, F.; Pan, H. Arrangement of landscape plants in parks of Shenzhen. *J. Northeast. For. Univ.* **2011**, *39*, 102–105.
48. Qiu, G.; Tan, S.; Wang, Y.; Yu, X.; Yan, C. Characteristics of evapotranspiration of urban lawns in a sub-tropical megacity and its measurement by the 'Three Temperature Model+ Infrared Remote Sensing'method. *Remote Sens.* **2017**, *9*, 502. [CrossRef]
49. Hao, G.Y.; Sack, L.; Wang, A.Y.; Cao, K.F.; Goldstein, G. Differentiation of leaf water flux and drought tolerance traits in hemiepiphytic and non-hemiepiphytic Ficus tree species. *Funct. Ecol.* **2010**, *24*, 731–740. [CrossRef]
50. Granier, A. Evaluation of transpiration in a Douglas-fir stand by means of sap flow measurements. *Tree Physiol.* **1987**, *3*, 309–320. [CrossRef]
51. Lundblad, M.; Lagergren, F.; Lindroth, A. Evaluation of heat balance and heat dissipation methods for sapflow measurements in pine and spruce. *Ann. For. Sci.* **2001**, *58*, 625–638. [CrossRef]
52. Delzon, S.; Sartore, M.; Granier, A.; Loustau, D. Radial profiles of sap flow with increasing tree size in maritime pine. *Tree Physiol.* **2004**, *24*, 1285–1293. [CrossRef]
53. Lu, P.; Urban, L.; Zhao, P. Granier's thermal dissipation probe (TDP) method for measuring sap flow in trees: Theory and practice. *Acta Bot. Sin.* **2004**, *46*, 631–646.
54. Oishi, A.C.; Hawthorne, D.A.; Oren, R. Baseliner: An open-source, interactive tool for processing sap flux data from thermal dissipation probes. *SoftwareX* **2016**, *5*, 139–143. [CrossRef]
55. Jarvis, P.G.; McNaughton, K.G. Stomatal control of transpiration: Scaling up from leaf to region. *Adv. Ecol. Res.* **1986**, *15*, 1–49.
56. Whitehead, D. Regulation of stomatal conductance and transpiration in forest canopies. *Tree Physiol.* **1998**, *18*, 633–644. [CrossRef]
57. Tetens, O. Uber einige meteorologische Begriffe. *Z. Geophys.* **1930**, *6*, 297–309.
58. Wang, H.; Zhao, P.; Hölscher, D.; Wang, Q.; Lu, P.; Cai, X.A.; Zeng, X.P. Nighttime sap flow of *Acacia mangium* and its implications for nighttime transpiration and stem water storage. *J. Plant Ecol.* **2012**, *5*, 294–304. [CrossRef]
59. Chu, X.; Han, G.; Xing, Q.; Xia, J.; Sun, B.; Yu, J.; Li, D. Dual effect of precipitation redistribution on net ecosystem CO_2 exchange of a coastal wetland in the Yellow River Delta. *Agric. For. Meteorol.* **2018**, *249*, 286–296. [CrossRef]
60. Van Gorsel, E.; Harman, I.N.; Finnigan, J.J.; Leuning, R. Decoupling of air flow above and in plant canopies and gravity waves affect micrometeorological estimates of net scalar exchange. *Agric. For. Meteorol.* **2011**, *151*, 927–933. [CrossRef]
61. Falge, E.; Baldocchi, D.; Olson, R.; Anthoni, P.; Aubinet, M.; Bernhofer, C.; Burba, G.; Ceulemans, R.; Clement, R.; Dolman, H. Gap filling strategies for long term energy flux data sets. *Agric. For. Meteorol.* **2001**, *107*, 71–77. [CrossRef]
62. Tang, Y.; Wen, X.; Sun, X.; Zhang, X.; Wang, H. The limiting effect of deep soil water on evapotranspiration of a subtropical coniferous plantation subjected to seasonal drought. *Adv. Atmos. Sci.* **2014**, *31*, 385–395. [CrossRef]
63. Jeon, J. The strengths and limitations of the statistical modeling of complex social phenomenon: Focusing on SEM, path analysis, or multiple regression models. *Int. J. Econ. Manag. Eng.* **2015**, *9*, 1634–1642.
64. Jia, X.; Zha, T.S.; Gong, J.N.; Wu, B.; Zhang, Y.Q.; Qin, S.G.; Peltola, H. Energy partitioning over a semi-arid shrubland in northern China. *Hydrol. Processes* **2016**, *30*, 972–985. [CrossRef]
65. Scholz, F.G.; Bucci, S.J.; Goldstein, G.; Meinzer, F.C.; Franco, A.C.; Miralles-Wilhelm, F. Removal of nutrient limitations by long-term fertilization decreases nocturnal water loss in savanna trees. *Tree Physiol.* **2007**, *27*, 551–559. [CrossRef]
66. Novick, K.A.; Oren, R.; Stoy, P.C.; Siqueira, M.B.S.; Katul, G.G. Nocturnal evapotranspiration in eddy-covariance records from three co-located ecosystems in the Southeastern US: Implications for annual fluxes. *Agric. For. Meteorol.* **2009**, *149*, 1491–1504. [CrossRef]
67. Guo, X.; Shang, G.; Tian, Y.; Jia, X.; Zha, T.; Li, C.; Zhang, X. Dynamics of Nocturnal Evapotranspiration and Its Biophysical Controls over a Desert Shrubland of Northwest China. *Forests* **2021**, *12*, 1296. [CrossRef]
68. Yan, C.; Guo, Q.; Li, H.; Li, L.; Qiu, G.Y. Quantifying the cooling effect of urban vegetation by mobile traverse method: A local-scale urban heat island study in a subtropical megacity. *Build. Environ.* **2020**, *169*, 106541. [CrossRef]

69. Montaldo, N.; Oren, R. The way the wind blows matters to ecosystem water use efficiency. *Agric. For. Meteorol.* **2016**, *217*, 1–9. [CrossRef]
70. Zhao, C.Y.; Si, J.H.; Feng, Q.; Yu, T.F.; Du Li, P. Comparative study of daytime and nighttime sap flow of *Populus euphratica*. *Plant Growth Regul.* **2017**, *82*, 353. [CrossRef]
71. Baldocchi, D.D.; Xu, L.; Kiang, N. How plant functional-type, weather, seasonal drought, and soil physical properties alter water and energy fluxes of an oak–grass savanna and an annual grassland. *Agric. For. Meteorol.* **2004**, *123*, 13–39. [CrossRef]
72. Wang, Q.; Gao, J.; Zhao, P.; Zhu, L.; Ouyang, L.; Ni, G.; Zhao, X. Biotic-and abiotic-driven variations of the night-time sap flux of three co-occurring tree species in a low subtropical secondary broadleaf forest. *AoB Plants* **2018**, *10*, ply025. [CrossRef]
73. Zhao, W.; Liu, B. The response of sap flow in shrubs to rainfall pulses in the desert region of China. *Agric. For. Meteorol.* **2010**, *150*, 1297–1306. [CrossRef]
74. Zhu, L.W.; Zhao, P. Temporal variation in sap-flux-scaled transpiration and cooling effect of a subtropical *Schima superba* plantation in the urban area of Guangzhou. *J. Integr. Agric.* **2013**, *12*, 1350–1356. [CrossRef]
75. Zha, T.; Barr, A.G.; van der Kamp, G.; Black, T.A.; McCaughey, J.H.; Flanagan, L.B. Interannual variation of evapotranspiration from forest and grassland ecosystems in western Canada in relation to drought. *Agric. For. Meteorol.* **2010**, *150*, 1476–1484. [CrossRef]
76. Alvarado-Barrientos, M.S.; Asbjornsen, H.; Holwerda, F. Is nighttime transpiration enhanced after fog events? *Acta. Hort.* **2013**, *991*, 133–139. [CrossRef]
77. Bucci, S.J.; Goldstein, G.; Meinzer, F.C.; Franco, A.C.; Campanello, P.; Scholz, F.G. Mechanisms contributing to seasonal homeostasis of minimum leaf water potential and predawn disequilibrium between soil and plant water potential in Neotropical savanna trees. *Trees* **2005**, *19*, 296–304. [CrossRef]
78. Cavender-Bares, J.; Sack, L.; Savage, J. Atmospheric and soil drought reduce nocturnal conductance in live oaks. *Tree Physiol.* **2007**, *27*, 611–620. [CrossRef]
79. Zeppel, M.; Tissue, D.; Taylor, D.; Macinnis-Ng, C.; Eamus, D. Rates of nocturnal transpiration in two evergreen temperate woodland species with differing water-use strategies. *Tree Physiol.* **2010**, *30*, 988–1000. [CrossRef]
80. Barbeta, A.; Ogaya, R.; Peñuelas, J. Comparative study of diurnal and nocturnal sap flow of Quercus ilex and Phillyrea latifolia in a Mediterranean holm oak forest in Prades (Catalonia, NE Spain). *Trees* **2012**, *26*, 1651–1659. [CrossRef]
81. Pfautsch, S.; Keitel, C.; Turnbull, T.L.; Braimbridge, M.J.; Wright, T.E.; Simpson, R.R.; Adams, M.A. Diurnal patterns of water use in *Eucalyptus victrix* indicate pronounced desiccation–rehydration cycles despite unlimited water supply. *Tree Physiol.* **2011**, *31*, 1041–1051. [CrossRef]
82. Kavanagh, K.L.; Pangle, R.; Schotzko, A.D. Nocturnal transpiration causing disequilibrium between soil and stem predawn water potential in mixed conifer forests of Idaho. *Tree Physiol.* **2007**, *27*, 621–629. [CrossRef]
83. Yoshifuji, N.; Kumagai, T.O.; Tanaka, K.; Tanaka, N.; Komatsu, H.; Suzuki, M.; Tantasirin, C. Inter-annual variation in growing season length of a tropical seasonal forest in northern Thailand. *For. Ecol. Manag.* **2006**, *229*, 333–339. [CrossRef]
84. Liu, H.; Park Williams, A.; Allen, C.D.; Guo, D.; Wu, X.; Anenkhonov, O.A.; Badmaeva, N.K. Rapid warming accelerates tree growth decline in semi-arid forests of Inner Asia. *Glob. Change Biol.* **2013**, *19*, 2500–2510. [CrossRef]
85. Wu, X.; Liu, H.; Li, X.; Liang, E.; Beck, P.S.; Huang, Y. Seasonal divergence in the interannual responses of Northern Hemisphere vegetation activity to variations in diurnal climate. *Sci. Rep.* **2016**, *6*, 19000. [CrossRef]
86. Ma, J.; Zha, T.; Jia, X.; Tian, Y.; Bourque, C.P.A.; Liu, P.; Chen, W. Energy and water vapor exchange over a young plantation in northern China. *Agric. For. Meteorol.* **2018**, *263*, 334–345. [CrossRef]
87. Xie, J.; Zha, T.; Zhou, C.; Jia, X.; Yu, H.; Yang, B.; Peltola, H. Seasonal variation in ecosystem water use efficiency in an urban-forest reserve affected by periodic drought. *Agric. For. Meteorol.* **2016**, *221*, 142–151. [CrossRef]
88. Wang, H.; Tetzlaff, D.; Dick, J.J.; Soulsby, C. Assessing the environmental controls on Scots pine transpiration and the implications for water partitioning in a boreal headwater catchment. *Agric. For. Meteorol.* **2017**, *240*, 58–66. [CrossRef]
89. Meinzer, F.C.; James, S.A.; Goldstein, G. Dynamics of transpiration, sap flow and use of stored water in tropical forest canopy trees. *Tree Physiol.* **2004**, *24*, 901–909. [CrossRef]
90. Verbeeck, H.; Steppe, K.; Nadezhdina, N.; de Beeck, M.O.; Deckmyn, G.; Meiresonne, L.; Janssens, I.A. Stored water use and transpiration in Scots pine: A modeling analysis with ANAFORE. *Tree Physiol.* **2007**, *27*, 1671–1685. [CrossRef]
91. Wang, H.; Tetzlaff, D.; Soulsby, C. Hysteretic response of sap flow in Scots pine (*Pinus sylvestris*) to meteorological forcing in a humid low-energy headwater catchment. *Ecohydrology* **2019**, *12*, e2125. [CrossRef]
92. Ewers, B.E.; Oren, R.; Phillips, N.; Strömgren, M.; Linder, S. Mean canopy stomatal conductance responses to water and nutrient availabilities in *Picea abies* and *Pinus taeda*. *Tree Physiol.* **2001**, *21*, 841–850. [CrossRef] [PubMed]